The locus of fixation and the foveal cone mosaic

Nicole M. Putnam* The Institute of Optics, University of Rochester, Rochester, NY, USA

Heidi J. Hofer Center for Visual Science and The Institute of Optics, University of Rochester, Rochester, NY, USA

Nathan Doble† Center for Visual Science, University of Rochester, Rochester, NY, USA

Li Chen Center for Visual Science, University of Rochester, Rochester, NY, USA

Joseph Carroll Center for Visual Science, University of Rochester, Rochester, NY, USA

David R. Williams Center for Visual Science and The Institute of Optics, University of Rochester, Rochester, NY, USA

High-resolution retinal imaging with adaptive optics was used to record the position of a light stimulus on the cone mosaic with an error at least five times smaller than the diameter of the smallest foveal cones. We discuss the factors that limit the accuracy with which absolute retinal position can be determined. In five subjects, the standard deviation of fixation positions measured in discrete trials ranged from 2.1 to 6.3 arcmin, with an average of 3.4 arcmin (about 17 μm), in agreement with previous studies (R. W. Ditchburn, 1973; R. M. Steinman, G. M. Haddad, A. A. Skavenski, & D. Wyman, 1973). The center of fixation, based on the mean retinal position for each of three subjects, was displaced from the location of highest foveal cone density by an average of about 10 arcmin (about 50 μm), indicating that cone density alone does not drive the location on the retina selected for fixation. This method can be used in psychophysical studies or medical applications requiring submicron registration of stimuli with respect to the retina or in delivering light to retinal features as small as single cells.

Keywords: physiological optics, eye movements, fixation, adaptive optics, cone density, fovea

Introduction

The most accurate methods to measure the motion of the retina with respect to the retinal image are those that track the retina itself (e.g., Cornsweet, 1958; Crossland & Rubin, 2002; Hammer et al., 2003). The development of adaptive optics instruments to image the retina at very high resolution provides access to microscopic structures as small as about 2 μm on the retina (Hofer et al., 2001; Liang, Williams, & Miller, 1997). In principal, the ability to image such features could make it possible to track movements of the retinal image with greater accuracy than has been possible before. Here we present a method to track retinal position with accuracy better than a fifth the size of the smallest foveal cone photoreceptor.

We demonstrate the value of this method by determining the relationship between the center of fixation and the topography of cones at the foveal center. Saccadic eye movements allow the observer to rapidly direct the acute fovea to locations of interest in visual scenes. It is usually assumed that the retinal location the visual system has chosen for fixation corresponds to the foveal center, where the density of cones is highest (Carpenter, 1991; Polyak, 1949). Although this assumption is approximately correct, we show here that the center of fixation can be displaced from the location of peak cone density in normal eyes.

Methods

Subjects

Five subjects with clinically normal vision and ranging in age from 22 to 30 years participated in the experiment after providing written consent in accordance with the Declaration of Helsinki. J.P., A.L., and D.G. had uncorrected vision, whereas J.C. (4 diopters) and NP (2.75 diopters) were myopic, but correctable to 20/20.

Procedure

The pupils of the subjects' right eyes were dilated with a drop of 2.5% phenylephrine and a drop of 1% tropicamide

doi: 10.1167/5.7.3 Received April 20, 2005; published August 17, 2005 ISSN 1534-7362

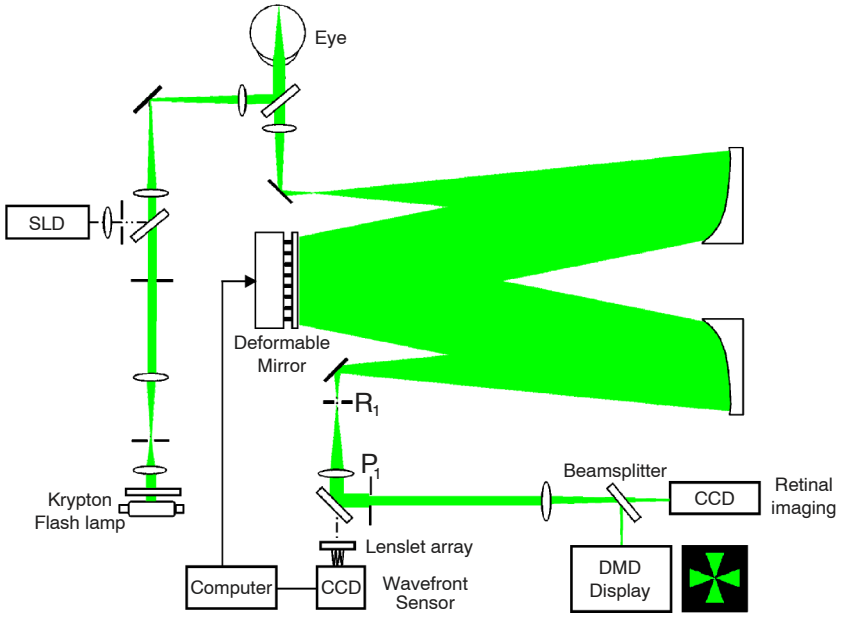

Figure 1. The Rochester adaptive optics ophthalmoscope. The target was a Maltese cross presented at 550 nm.

before data collection. A dental impression was used to stabilize the subject's head. Each subject's task was to fixate a Maltese cross (shown in Figure 1) displayed on a digital micromirror device (Texas Instruments, Dallas, TX) and viewed through a 6-mm artificial pupil. The Maltese cross subtended 1° visual angle and was viewed with a 550-nm light at 390 Trolands. All subjects were given time to acclimate to the optical instrument and practice the task. When the subject felt they were fixating accurately, they initiated a sequence of events that resulted in delivery of a light flash for acquiring a high-resolution retinal image as described later. The light flash was 4 ms in duration and has the same wavelength (550 nm) as the fixation stimulus. Its energy was typically 0.6 μJ delivered through a 2.5-mm pupil. These images allowed us to determine the location of the stimulus on the retina on each flash. On a small percentage of flashes, less than 5% of the time, a saccade blurred the image. These trials were discarded. Between 69 and 119 images were used for analysis, depending on the subject. The imaging flash generated an afterimage that tended to disrupt fixation. To avoid this, subjects were instructed to wait until the afterimage had disappeared before initiating the next trial.

Retinal imaging

Figure 1 shows a schematic diagram of the Rochester adaptive optics ophthalmoscope similar to that described by Hofer et al. (2001) except for the use of a deformable mirror with 97 actuators instead of 37. A high-quality pellicle beamsplitter with an optical flatness better than $\lambda/10$ allowed the subject to view the fixation stimulus while also allowing the light from the imaging flash into the retinal-imaging camera. A 9 : 1 ratio of transmittance to reflectance was used to minimize loss of light in the retinal image.

The subject's optical aberrations were measured with a Shack-Hartmann wavefront sensor and corrected with a deformable mirror (Xinetics, Devins, MA). Wavefront sensing was performed with a 820-nm light from a superluminescent diode. The superluminescent diode was positioned at the perimeter of the Maltese cross stimulus, so as not to interfere with fixation. The wave aberration was measured and the deformable mirror corrected the wave aberration in an iterative manner, at a frame rate of 30 Hz, corresponding to a closed-loop bandwidth of about 1 Hz.

The flashlamp was automatically triggered once a desired root-mean-square wavefront aberration was achieved ($\approx$0.1 μm over a 6.8-mm pupil) or once 10 cycles of measurement and correction had been completed, whichever occurred first. In either case, this took less than one third of a second. The retinal image was acquired with a cooled CCD camera (Roper Scientific, Trenton, NJ). Although wavefront correction was performed over a 6.8-mm pupil, the light for the retinal images was collected only over the central 6 mm to reduce edge artifacts in aberration correction.

The delay of less than one third of a second between the subject's initiation of the flash and its occurrence did not influence the accuracy of fixation. Control experiments (data not shown) in which the adaptive correction was running continuously and the flash was presented immediately following the subject's button press revealed that this delay had no measurable influence on the accuracy of fixation.

Fixation stimulus and CCD alignment

The use of retinal images to measure the location of fixation depends on accurate alignment of the fixation stimulus relative to the CCD camera. A plane mirror was placed in a

retinal-conjugate plane (R_1), which allowed the fixation target to be imaged directly on the CCD camera. The fixation target and CCD were aligned horizontally and vertically so that the center of the fixation target fell at the center of the 512×512 CCD array. This alignment procedure locked the relative positions of the fixation target and the retinal-imaging camera, even if the subject's pupil moved with respect to the optical system.

Retinal image analysis

The fixation position on each trial was given by the retinal location that lay at the center of the CCD image. The movement of the retinal image from trial to trial was computed from the relative displacement of the cone photoreceptors in retinal images. First, images were bilinearly interpolated by a factor of 4 and then spatially filtered with a difference of Gaussian filter (σ_{center} = 0.12 arcmin, $\sigma_{surround}$ = 0.85 arcmin) to remove the low frequency components corresponding to the edge of the imaging field and the high frequency noise above the diffraction limited cutoff frequency of the eye's optics. These processed images were then cross-correlated to determine the horizontal and vertical translation, achieving subpixel registration.

Measuring cone spacing

For three subjects (J.P., A.L., and J.C.) we created montages of a large area of central retina (1–2.5° diameter). A freely available image-processing program (*Image J*, National Institutes of Health, Bethesda, MD) was used to manually identify the cones in each montage. The (x,y) coordinates of the cones were stored in a text array and cone density was estimated using a custom MatLab (MathWorks, Natick, MA) algorithm. To calculate cone density, we used a sampling technique outlined by Curcio, Sloan, Kalira, and Hendrickson (1990). The list of cone coordinates was scanned with a sampling window with a radius of 20.6 μm (the position of the sampling window was incremented/decremented by multiples of the window radius). At each location, the number of cones within the sampling window was recorded. The area of retina sampled at each point approximately 1300 μm^2. By dividing the number of cones by the area of the sampling window, we derived an estimate of cone density at each window location. From this data set, a contour plot was created. Rather than assigning the absolute peak density as the foveal center, we found the center of each of six isodensity contour lines (representing between 80% and 93% of the peak cone density value). These values were averaged, and the resulting value was estimated to be the foveal center, based specifically on this analysis of cone density. Axial length measurements made with an IOL master (Carl Zeiss Meditec, Inc., Dublin, CA) allowed accurate conversions from minutes of visual angle to microns on the retina for each subject.

Results and discussion

Sources of error in measuring eye position

Accuracy of cross-correlation

Figure 2 shows a typical one-dimensional cross-section through the two-dimensional cross-correlation function of a pair of retinal images. The function has a maximum indicating the displacement (d) required to bring the images into register. The original 512×512 images were linearly interpolated by a factor of 4, corresponding to an interpolated pixel size of approximately 0.03 arcmin. The pixel corresponding to the peak of the cross-correlation function is readily identifiable, and the displacement corresponding to this pixel determined the retinal image movement between images. More sophisticated methods such as fitting the peak of the cross-correlation function with a Gaussian could have reduced the registration error by several orders of magnitude. However, other sources of error were large enough that there was no motivation to use a more nearly precise method.

Figure 2 shows that even with our simple method of identifying the displacement, the shift between images can be determined with an error that is 4 times smaller than the wavelength of light, 16 times smaller the diameter a foveal cone, and 13 times smaller than the full width half-maximum of the diffraction-limited point-spread function of the eye with a 6-mm pupil.

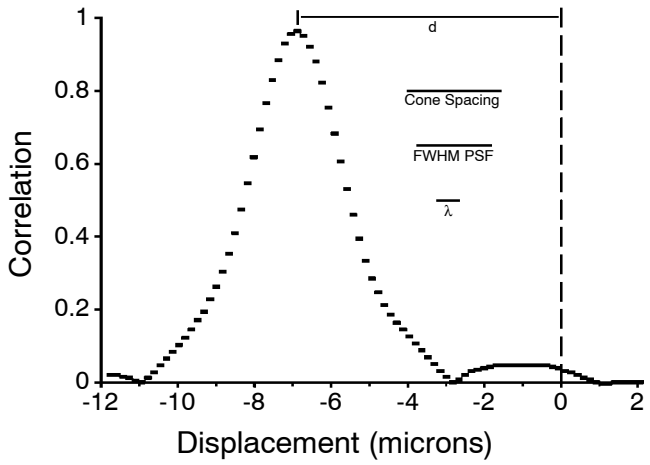

Figure 2. Cross-section through the two-dimensional cross-correlation function of a pair of retinal images. The width of the data points in the cross-section indicate the width of an interpolated pixel, or one fourth of the width of a pixel of the CCD camera. The displacement (d) of the peak of the function from the origin provides the translation in one dimension. Lines to the right of the plot represent the row-row spacing of cones in these retinal images, the full width half-maximum of a diffraction-limited point-spread function at 550 nm, and the wavelength of light.

Eye motion during the exposure

Another limitation on the accuracy of the method is the motion of the eye during a single exposure. We used a 4-ms exposure to give us the largest signal per flash while keeping images that were visibly blurred by eye motion to fewer than about 5%. Riggs, Armington, and Ratliff (1954) reported median retinal image motion as a function of stimulus duration from about 15 ms to 1 s. Extrapolation of their data down to 4 ms predicts a median retinal image motion of 1.5 arcsec, which is one twentieth of the size of a foveal cone. Because we rejected trials in which there was visible motion blur corresponding to saccades, we conclude that retinal image motion is not an important limitation.

Head stabilization and axial alignments

The fixation stimulus and the CCD should be aligned so that they occupy conjugate planes and are in focus on the retina simultaneously. An error in focus of one relative to the other will introduce errors in estimating the point of fixation because of parallax if the head translates relative to the optical system. The angular parallax, Θ, is given by

$$\Theta = \arctan(x \bullet |\triangle D|) \quad (1)$$

where x is the lateral displacement of the head in meters and $\triangle D$ is the dioptric difference in focus between the stimulus and the CCD. Pupil displacements when sitting in the bite bar are highly subject dependent. Makous (1998) reported the pupil of experienced subjects clenching a bite bar typically stays within 50 μm of its intended position. We did not obtain records of pupil movement, so assume conservatively a standard deviation for pupil movement of 200 μm. For a conservative focus error as large as 0.1 diopters, the parallax at the retina would be only about 0.07 arcmin, or one eighth of the diameter of a foveal cone. Parenthetically, we used monochromatic light of the same wavelength for both imaging and fixation to avoid additional parallax caused by head movements in conjunction with the chromatic aberration of the eye.

Combining the errors associated with cross-correlation, eye motion during the exposure, and head instability on the bite bar, the total error in the measurement of the fixational stability is at most 0.08 arcmin, or one sixth the size of a single foveal cone photoreceptor. This error corresponds to about 400 nm at the retina, which is less than the wavelength of our stimulus. This accuracy could be improved if the demands required it by more careful head stabilization and alignment procedures, briefer imaging flashes, and a more sophisticated method of locating image cross-correlation peaks.

Lateral alignment error

There is one additional source of error, which is the accuracy with which the fixation stimulus is registered with respect to the CCD array. Assuming a conservative error as large as 0.5 of a retinal image pixel, this would cause an error of approximately 0.06 arcmin, or about one eighth of the diameter of a foveal cone. This is a systematic error in our ability to determine absolute fixation position and does not result in any error in determining the relative shift in position from one fixation to the next. This error combined with the other sources of error results in a total error in determining the absolute position of a stimulus on the retina of about 0.1 arcmin, or approximately one fifth of the diameter of a foveal cone.

Fixation stability

Figure 3 shows fixation locations for 83 trials superimposed on the foveal cone mosaic for one subject (J.P.). The cross shows the mean fixation position and the ellipses correspond to one and two standard deviations.

Similar results were obtained on the other four subjects. The standard deviation ranged from 2.1 to 6.3 arcmin (10.2–30.9 μm) in the vertical and horizontal directions, with an average of 3.6 arcmin (17.8 μm) in the horizontal direction and 3.2 arcmin (15.6 μm) in the vertical direction. Table 1 shows the data for all five subjects. Except for one instance (D.G., vertical direction) fixation points were normally distributed in both the vertical and horizontal dimension, based on the Kolmogorov-Smirnov

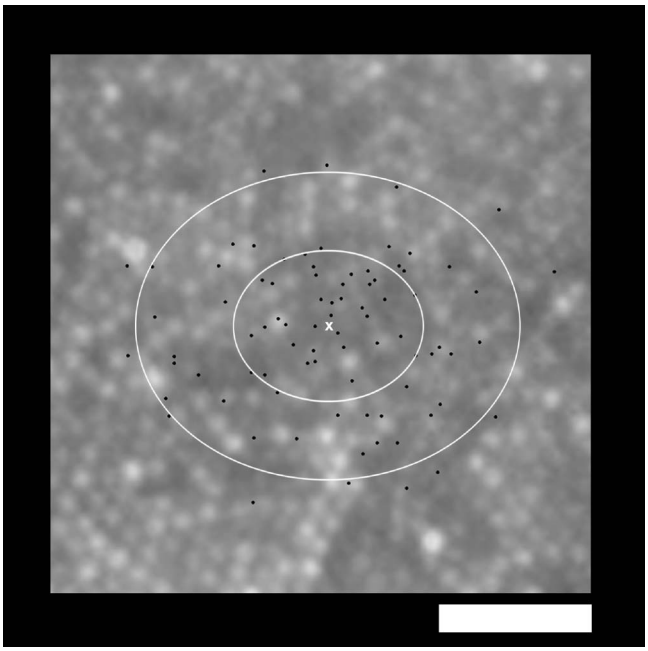

Figure 3. The foveal cone mosaic for one subject (J.P.) with the location of 83 fixations superimposed (small black dots). The size of the dots corresponds to the error of measurement, which is estimated to be about 5 arcsec. The white cross is the average fixation position. The foveal center (area of highest cone density) does not appear in this image, but resides 59.5 μm temporal inferior (up and to the right) of the average fixation position. White ellipses represent ±1 and ±2 standard deviations for fixation. Scale bar is 20 μm (4.03 arcmin).

Subject	Horizontal standard deviation of fixation (arcmin : μm)	Vertical standard deviation of fixation (arcmin : μm)	Mean standard deviation of fixation (arcmin : μm)	Peak cone density (cones/mm^2)	Deviation of center of fixation from the foveal center (μm)
J.P.	2.56 : 12.7	2.06 : 10.2	2.31 : 11.5	148,825	36.48 nasal, 47.00 superior
N.P.	6.30 : 30.9	3.29 : 16.1	4.80 : 23.5	—	—
D.G.	3.18 : 15.0	5.49 : 25.9	4.33 : 20.5	—	—
A.L.	3.26 : 16.1	2.58 : 12.7	2.92 : 14.4	114,963	18.49 temporal, 44.40 superior
J.C.	2.62 : 14.5	2.38 : 13.2	2.50 : 13.8	226,929	44.08 temporal, 12.80 inferior
Average	3.58 : 17.8	3.16 : 15.6	3.37 : 16.7	163,572	—

Table 1. Summary of data relating fixational stability and the relationship between cone density and the center of fixation.

test for normality ($p > .10$). This is consistent with previous findings (Steinman, 1965).

These results are in agreement with previous reports that used a variety of methods. For example, Barlow (1952) estimated a standard deviation of approximately 5 arcmin. Ditchburn (1973) reported the standard deviation ranges from 1.4 to 3.2 arcmin for subjects fixating at a distant target, and Steinman et al. (1973) reported standard deviations ranging from approximately 2 to 5 arcmin during maintained fixation. These earlier reports of the stability of gaze were based on measurements of the front of the eye. The data reported here have the advantage that the retina itself was directly tracked. The agreement between the front and the back of the eye tracking methods tends to suggest that both approaches generate accurate estimates of the stability of gaze.

Fixation location and cone topography

Despite the miniature eye movements that characterize the fixating eye, the prevailing view is that the eye has a quite small and stable preferred retinal locus of fixation (Barlow, 1952; Steinman, 1965). Steinman (1965) reported that the location of fixation can shift about 2 arcmin depending on target size, color, and luminance but concluded that these small shifts did not vitiate the notion of a stable retinal location for fixation. An assumption that is almost universally adopted is that the center of fixation corresponds to the anatomical center of the fovea (Polyak, 1949). Displacements between the two are generally associated with vision loss, as in the development of a pseudofovea in macular degeneration (Timberlake et al., 1986; von Noorden & Mackensen, 1962; White & Bedell, 1990) In normal eyes, however, the terms *center of fixation* and *center of the fovea* are often used interchangeably in psychophysical experiments. High-resolution imaging with adaptive optics provides an accurate measurement of whether the center of fixation actually does lie at the location of maximum cone density.

Figure 4 shows scatter plots of fixation superimposed on the cone mosaic for three of the five subjects. The remaining two subjects are not included because of the difficulty resolving cones at the foveal center (and thereby impeding accurate estimates of cone density). The black squares show the center of the area of highest cone density for each subject. Peak cone density values were the following: J.P. = 148,825 cones/mm^2; A.L. = 114,963 cones/mm^2; J.C. = 226,929 cones/mm^2. The dashed and solid lines are contours representing a 5% and 15% increase in cone spacing, respectively. Note that for each subject, the mean fixation position is displaced from the anatomical foveal center, defined by cone density. The displacements are the following: J.P., 59.5 μm (11.26 arcmin) nasal superior; A.L., 48.1 μm (9.75 arcmin) temporal superior; J.C., 45.9 μm (8.29 arcmin) temporal from the foveal center. Table 1 gives the two-dimensional vector displacements for each subject. Depending on the observer, the center of fixation lies approximately three to five times further from the point of highest cone density than the standard deviation of fixation. The direction of the displacement does not appear to be systematic, although more subjects would be required to confirm this.

Besides the location of maximum cone density, there are other anatomical features that can be used to define the foveal center, such as the foveal pit, the avascular zone, the rod-free zone, and the tritanopic zone. Curcio et al. (1991, 1990) reported that neither the rod-free zone nor the tritanopic zone is perfectly centered on the location of peak cone density. Bedell (1980) and Zeffren, Applegate, Bradley, and van Heuven (1990) reported that fixation position is not always symmetrically placed within the foveal avascular zone. Although Bedell (1980) reported a deviation of 0.6–0.8° in one eye, Zeffren et al. (1990) found that on average, the center of fixation deviated 66.5 ± 49.5 μm from the center of the avascular zone.

Under the somewhat dubious assumption that acuity is reciprocally related to cone spacing near the fovea (Green, 1970; Marcos & Navarro, 1997), acuity will have declined by 8.2%, 4.4%, and 10.1% for J.P., A.L., and J.C., respectively, at the center of fixation compared with the anatomic center of the fovea. The displacement results, therefore, predict relatively small losses in acuity. Although it is thought that acuity generally falls in all directions away from the center of fixation, there have been few measurements that address whether this holds true within the central foveal region (Clemmesen, 1944; Jones & Higgins, 1947; Weymouth, Hines, Acres, Raaf, & Wheeler, 1928). Weymouth et al. (1928) mapped grating acuity in 11 arcmin steps throughout the fovea in three observers and did not report that the location of maximum acuity was displaced from fixation. However, blurring by the eye's optics reduces foveal visual acuity somewhat below the cone Nyquist frequency (Marcos & Navarro, 1997), which tends to obscure the influence of cone density. It would be of some interest to revisit the relationship between the spatial variation in

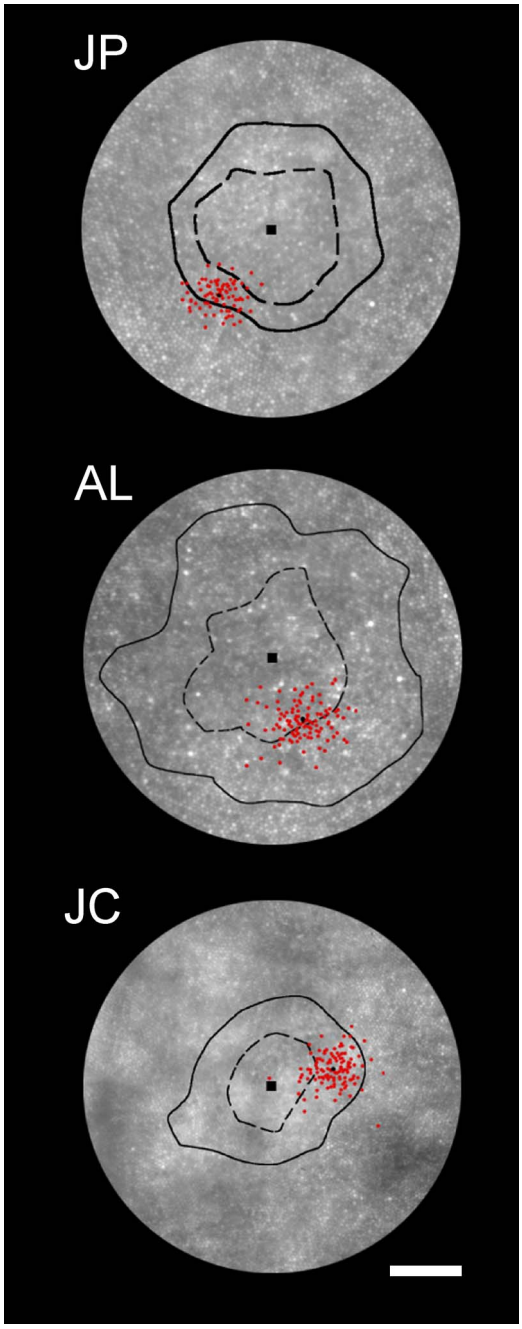

Figure 4. Area of highest cone density is not always used for fixation. Shown are retinal montages of the foveal cone mosaic for three subjects. The black square represents the foveal center of each subject (see the Methods section for how this was derived). The dashed black line is the isodensity contour line representing a 5% increase in cone spacing, and the solid black line is the isodensity contour line representing a 15% increase in cone spacing. Red dots are individual fixation locations. Scale bar is 50 μm.

acuity and cone density across the central fovea using interference fringe stimuli that are immune to optical blur.

Although the eye's optical blur may relax the pressure to select a center of fixation precisely at the location of highest cone density, the possibility remains that other factors may drive the fixation locus. The variation in optical quality of the cornea and lens with retinal eccentricity is not a viable candidate for driving fixation because it changes so slowly (Jennings & Charman, 1981; Navarro, Artal, & Williams, 1993; Williams, Artal, Navarro, McMahon, & Brainard, 1996). It seems hard to escape the conclusion that the foveal pit and its associated avascular zone evolved to provide superior optical quality to foveal cones (Polyak, 1949; Weale, 1966), despite the fact that a difference in optical quality has proven difficult to measure (Artal & Navarro, 1992; Williams, Brainard, McMahon, & Navarro, 1994). It is conceivable that fixation coincides with the bottom of the foveal pit, and that both can be shifted from the cone density peak. Alternatively, the relatively small offsets observed here might simply reflect the insensitivity of the biological process with which fixation is established. If this were true, then left unexplained is the small standard deviation of fixation. The deleterious consequences of motion of the retinal image caused by fixation variability, such as the loss of vision during saccades (Dodge, 1900), may drive the visual system to keep fixation variability small.

Applications of tracking retinal position with subphotoreceptor accuracy

The present study capitalizes on the high spatial resolution afforded by adaptive optics to provide an instantaneous estimate of eye position with accuracy of about 5 arcsec, or one fifth of the diameter of a foveal cone. This error is lower than previous methods of measuring eye position. For example, the accuracy of dual Purkinje eye tracking is about 1 arcmin (Cornsweet & Crane, 1973; Crane & Steele, 1978). In this method, displacements of the lens during saccades interfere with direct access to the motion of the image with respect to the retina (Deubel & Bridgeman, 1995). Scleral search coils are subject to movement, and the accuracy is also on the order of 1 arcmin (De Bie, 1985). The method described here has the advantage shared with all retinal tracking methods (e.g., Cornsweet, 1958; Crossland & Rubin, 2002; Hammer et al., 2003) that it tracks the retina directly, rather than other features of the eye. Our method also has the advantage of revealing the absolute position of the stimulus on the retina.

So far, we have been able to record retinal location only for brief instants in time. However, Roorda et al. (2002) have coupled adaptive optics to a scanning laser ophthalmoscope with higher temporal bandwidth. Recently, they have demonstrated that they can use displacements of microscopic features such as photoreceptors from frame to frame to reconstruct the record of eye movements with much greater fidelity than previously possible (Stevenson, Raghunandan, Frazier, Poonja, & Roorda, 2004). This method of tracking the retina could also be used to increase precision in laser retinal surgery, such as photocoagulation used to treat diabetic retinopathy, resulting in less damage to healthy retinal tissue and ultimately, better outcomes for the patient.

There are many applications that would benefit from a more accurate method of measuring fixation. For example, it would be

possible to determine the contributions that individual receptors make to visual perception. There has been a long history of studies concerning the detection and appearance of small flashes of light (Cicerone & Nerger, 1989; Hartridge, 1947; Hofer, Singer, & Williams, 2005; Krauskopf, 1978; Vimal, Pokorny, Smith, & Shevell, 1989; Wesner, Pokorny, Shevell, & Smith, 1991; Williams, MacLeod, & Hayhoe, 1981). A shortcoming of these studies has been the inability to determine precisely the retinal location used for detection. Unpublished work in our laboratory has shown that it is possible to image the cone mosaic with infrared light that is invisible to the subject. This could enable psychophysical experiments where the specific cones or cones responsible for detecting a given stimulus can be identified unobtrusively on each presentation.

Acknowledgments

This research was supported by National Institutes of Health grants R01EY04367 and P30EY01319. This work has also been supported by the National Science Foundation Science and Technology Center for Adaptive Optics, managed by the University of California at Santa Cruz under cooperative agreement number AST-9876783.

Commercial relationships: none.
Corresponding author: David R. Williams.
Email: david@cvs.rochester.edu
[*]Currently at Optical Sciences Center, University of Arizona, Tucson, AZ 85721.
[†]Currently at Iris AO Inc, 2680 Bancroft Way, Berkeley, CA 94704.

References

Artal, P., & Navarro, R. (1992). Simultaneous measurement of two point-spread functions at different locations across the human fovea. *Applied Optics, 31*(19), 3646–3656.

Barlow, H. B. (1952). Eye movements during fixation. *Journal of Physiology (London), 116*(3), 290–306. [PubMed]

Bedell, H. E. (1980). A functional test of foveal fixation based upon differential cone directional sensitivity. *Vision Research, 20*(6), 557–560. [PubMed]

Carpenter, R. H. S. (1991). The visual origins of ocular motility. In R. H. S. Carpenter (Ed.), *Eye movements* (Vol. 8, pp. 1–12). Boca Raton, FL: CRC Press.

Cicerone, C. M., & Nerger, J. L. (1989). The relative numbers of long-wavelength-sensitive to middle-wavelength-sensitive cones in the human fovea centralis. *Vision Research, 29*(1), 115–128. [PubMed]

Clemmesen, V. (1944). Central and indirect vision. *Acta Physiologica Scandinavia, 9*(Suppl. 27), 115–119.

Cornsweet, T. N. (1958). New technique for the measurement of small eye movements. *Journal of the Optical Society of America, 48*(11), 808–811. [PubMed]

Cornsweet, T. N., & Crane, H. D. (1973). Accurate two-dimensional eye tracker using first and fourth Purkinje images. *Journal of the Optical Society of America, 63*(8), 921–928. [PubMed]

Crane, H. D., & Steele, C. M. (1978). Accurate three-dimensional eyetracker. *Applied Optics, 17*(5), 691–714.

Crossland, M. D., & Rubin, G. S. (2002). The use of an infrared eyetracker to measure fixation stability. *Optometry and Vision Science, 79*(11), 735–739. [PubMed]

Curcio, C. A., Allen, K. A., Sloan, K. R., Lerea, C. L., Hurley, J. B., Klock, I. B., et al. (1991). Distribution and morphology of human cone photoreceptors stained with anti-blue opsin. *The Journal of Comparative Neurology, 312*, 610–624. [PubMed]

Curcio, C. A., Sloan, K. R., Kalina, R. E., & Hendrickson, A. E. (1990). Human photoreceptor topography. *The Journal of Comparative Neurology, 292*, 497–523. [PubMed]

De Bie, J. (1985). An afterimage vernier method for assessing the precision of eye movement monitors: Results for the scleral coil technique. *Vision Research, 25*(9), 1341–1343. [PubMed]

Deubel, H., & Bridgeman, B. (1995). Fourth Purkinje image signals reveal eye-lens deviations and retinal image distortions during saccades. *Vision Research, 35*(4), 529–538. [PubMed]

Ditchburn, R. W. (1973). *Eye-movements and visual perception.* Oxford: Clarendon Press.

Dodge, R. (1900). Visual perception during eye movement. *Psychological Review, 7,* 454–465.

Green, D. G. (1970). Regional variations in the visual acuity for interference fringes on the retina. *Journal of Physiology (London), 207*(2), 351–356. [PubMed]

Hammer, D. X., Ferguson, D. C., Magill, J. C., White, M. A., Elsner, A. E., & Webb, R. H. (2003). Compact scanning laser ophthalmoscope with high-speed retinal tracker. *Applied Optics, 42*(22), 4621–4632. [PubMed]

Hartridge, H. (1947). The visual perception of fine detail. *Philosophical Transactions of the Royal Society of London. Series B, Biological Sciences, 232*(592), 519–671.

Hofer, H., Chen, L., Yoon, G. Y., Singer, B., Yamauchi, Y., & Williams, D. R. (2001). Improvement in retinal image quality with dynamic correction of the eye's aberrations. *Optics Express, 8*(11), 631–643. [Article]

Hofer, H., Singer, B., & Williams, D. R. (2005). Different sensations from cones with the same photopigment. *Journal of Vision*, *5*(5), 444-454, http://journalofvision.org/5/5/5/, doi:10.1167/5.5.5. [PubMed] [Article]

Jennings, J. A., & Charman, W. N. (1981). Off-axis image quality in the human eye. *Vision Research, 21*(4), 445–455. [PubMed]

Jones, L. A., & Higgins, G. C. (1947). Photographic granularity and graininess. III. Some characteristics of the visual system of importance in the evaluation of graininess and granularity. *Journal of the Optical Society of America, 37*(4), 217–263.

Krauskopf, J. (1978). On identifying detectors. In A. J. C. Armington, J. Krauskopf, & B. R. Wooten (Eds.), *Visual psychophysics and physiology* (pp. 283–298). New York: Academic Press.

Liang, J., Williams, D. R., & Miller, D. (1997). Supernormal vision and high-resolution retinal imaging through adaptive optics. *Journal of the Optical Society of America A, 14*(11), 2884–2892. [PubMed]

Makous, W. (1998). Optics and photometry. In R. H. S. Carpenter & J. G. Robson (Eds.), *Vision research: A practical guide to laboratory methods* (pp. 1–49). Oxford: Oxford University Press.

Marcos, S., & Navarro, R. (1997). Determination of the foveal cone spacing by ocular speckle interferometry: Limiting factors and acuity predictions. *Journal of the Optical Society of America A, 14*(4), 731–740. [PubMed]

Navarro, R., Artal, P., & Williams, D. R. (1993). Modulation transfer of the human eye as a function of retinal eccentricity. *Journal of the Optical Society of America A, 10*(2), 201–212. [PubMed]

Polyak, S. (1949). Retinal structure and color vision. In F. P. Fischer, A. J. Schaeffer & A. Sorsby (Eds.), *Documenta Ophthalmologica: Advances in Ophthalmology* (Vol. 3, pp. 24–46). The Hague, Netherlands: Dr. W. Junk.

Riggs, L. A., Armington, J. C., & Ratliff, F. (1954). Motions of the retinal image during fixation. *Journal of the Optical Society of America, 44*(4), 315–321. [PubMed]

Roorda, A., Romero-Borja, F., Donnelly III, W. J., Quenner, H., Hebert, T. J., & Campbell, M. C. W. (2002). Adaptive optics scanning laser ophthalmoscopy. *Optics Express, 10*(9), 405–412. [Article]

Steinman, R. M. (1965). Effect of target size, luminance, and color on monocular fixation. *Journal of the Optical Society of America, 55*(9), 1158–1165.

Steinman, R. M., Haddad, G. M., Skavenski, A. A., & Wyman, D. (1973). Miniature eye movement. *Science, 181*(102), 810–819. [PubMed]

Stevenson, S. B., Raghunandan, A., Frazier, J., Poonja, S., & Roorda, A. (2004). Fixation jitter, motion discrimination and retinal imaging [Abstract]. *Journal of Vision, 4*(11), 85a, doi:10.1167/4.11.85, http://journalofvision.org/4/11/85/.

Timberlake, G. T., Mainster, M. A., Peli, E., Augliere, R. A., Essock, E. A., & Arend, L. E. (1986). Reading with a macular scotoma I. Retinal location of scotoma and fixation area. *Investigative Ophthalmology & Visual Science, 27*(7), 1137–1147. [PubMed]

Vimal, R. L. P., Pokorny, J., Smith, V. C., & Shevell, S. K. (1989). Foveal cone thresholds. *Vision Research, 29*(1), 61–78. [PubMed]

von Noorden, G. K., & Mackensen, G. (1962). Phenomenology of eccentric fixation. *American Journal of Ophthalmology, 53*, 642–660. [PubMed]

Weale, R. A. (1966). Why does the human retina possess a fovea? *Nature (London), 212*, 255–256. [PubMed]

Wesner, M. F., Pokorny, J., Shevell, S. K., & Smith, V. C. (1991). Foveal cone detection statistics in color-normals and dichromats. *Vision Research, 31*(6), 1021–1037. [PubMed]

Weymouth, F. W., Hines, D. C., Acres, L. H., Raaf, J. E., & Wheeler, M. C. (1928). Visual acuity within the area centralis and its relation to eye movements and fixation. *American Journal of Ophthalmology, 11*(12), 947–960.

White, J. M., & Bedell, H. E. (1990). The oculomotor reference in humans with bilateral macular disease. *Investigative Ophthalmology & Visual Science, 31*(6), 1149–1161. [PubMed]

Williams, D. R., Artal, P., Navarro, R., McMahon, M. J., & Brainard, D. H. (1996). Off-axis optical quality and retinal sampling in the human eye. *Vision Research, 36*(8), 1103–1114. [PubMed]

Williams, D. R., Brainard, D. H., McMahon, M. J., & Navarro, R. (1994). Double-pass and interferometric measures of the optical quality of the eye. *Journal of the Optical Society of America A, 11*(12), 3123–3135. [PubMed]

Williams, D. R., MacLeod, D. I. A., & Hayhoe, M. M. (1981). Punctate sensitivity of the blue-sensitive mechanism. *Vision Research, 21*(9), 1357–1375. [PubMed]

Zeffren, B. S., Applegate, R. A., Bradley, A., & van Heuven, W. A. J. (1990). Retinal fixation point location in the foveal avascular zone. *Investigative Ophthalmology & Visual Science, 31*(10), 2099–2105. [PubMed]